Characterisation of Dueodde, Denmark's 8th meteorite

MIA R.E. BOOTHROYD, CHARLOTTE R. HÅKANSSON, ANNA W. JENSEN, RASMUS ANDREASON & JAMES M. SCOTT

Boothroyd, M.R.E, Håkansson, C.R., Jensen, A.W., Andreason R. & Scott, J.M. 2026. Characterisation of Dueodde, Denmark's 8th meteorite. Bulletin of the Geological Society of Denmark, Vol. 75, pp. 215–222. ISSN 2245-7070. https://doi.org/10.37570/bgsd-2026-75-11

Geological Society of Denmark
https://2dgf.dk

Received 12 May 2026
Accepted in revised form 22 June 2026
Published online 10 August 2026

In 2017 a 75 g meteorite was recovered from a roof cavity of a summer house annex at Dueodde on the Danish island of Bornholm. Although the fall of Denmark's 8th recovered meteorite was not witnessed, the meteorite could have only resided there for a few years due to the age of the annex. We report the first detailed micro-analytical analysis of the mineral textures and mineral chemistries of this little-studied meteorite and attempt to classify the class, metamorphic grade and weathering state. Dueodde is a small, slightly abraded fusion-encrusted meteorite that has a pale medium to coarse-grained orthopyroxene-olivine-plagioclase-metal-rich interior. The compositional range of olivine (Fa_{16-20}; where Fa = 100*Fe/(Fe+Mg)) and orthopyroxene (Fs_{17-18}; where Fs = 100*Fe/(Fe+Mg)) in matrix and chondrules confirms Dueodde to be an H class ordinary chondrite. Chemical element maps highlight the occurrence of barred, radial and porphyritic chondrules, some of which are up to c. 3 mm in diameter. These maps also reveal that all three types of chondrule are distinctly depleted in metal minerals compared to the matrix, with this texture interpreted to represent metal expulsion during chondrule formation prior to incorporation and metamorphism in the parent body. The preservation of chondrule textures, the small variation in olivine Fa across the entire sample, and the plagioclase compositions suggest that Dueodde experienced metamorphism of grade 5 whilst in the parent body.

Keywords: Meteorite, H5, Bornholm, classification

Mia R.E. Boothroyd, Charlotte R. Håkansson, Anna W. Jensen, Rasmus Andreason, James M. Scott [jscott@geo.au.dk], Department of Geoscience, Aarhus University, Høegh-Guldbergs Gade 2, Aarhus, Denmark.

A meteorite was discovered at Dueodde in southern Bornholm in 2017, a place better known for its sandy beaches than its extraterrestrial material. The meteorite was found in the roof of an annex of a summerhouse, after a small hole of around 5 cm was discovered. The meteorite could have only fallen within the past couple of years prior to 2017 since the annex was only two to three years old.

Dueodde has had solely a brief characterisation to date and there are no published data. The stone, which is rounded and has a thin fusion crust, weighs 75 g (Fig. 1). The main mass is stored in Copenhagen at the Statens Naturhistoriske Museum, who loaned a small fragment for analysis. The existing classification, presented on the Meteoritical Bulletin (https://www.lpi.usra.edu), suggests that it is an H5 - a high iron ordinary chondrite (H) that experienced moderate to high metamorphism (grade 5). With recent microanalytical summaries of the Danish Meteorites Ejby (H5/6) by Haack *et al.* (2019) and Aarhus (H6) by Pedersen *et al.* (2025) now available to the public, we present a short summary, via microXRF and scanning electron microscope analysis, of textures and minerals preserved in Denmark's 8th known meteorite and a brief comparison to the aforementioned Ejby and Aarhus.

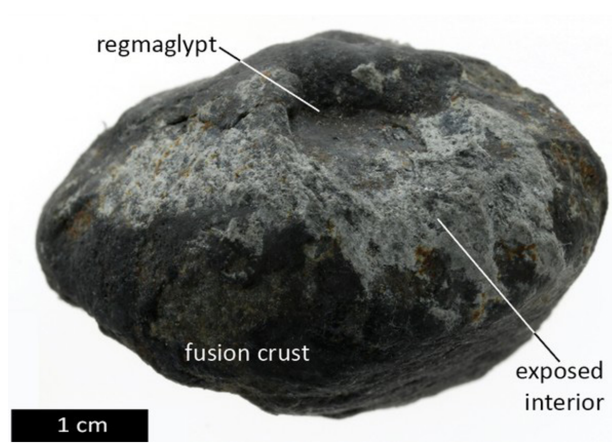

Fig. 1. Image of Dueodde taken before a slice was extracted. Used with permission from Martin Bizarro. Some of the pale surface displays a little bit of brown oxidation.

Methods

The provided flat slice of Dueodde was repolished to reduce surface roughness using diamond paste and polishing pads. One area in the center (Fig. 2a) remains unpolished where the diamond-saw dug into the surface. Micro-X-ray fluorescence (XRF) images were obtained using a BrukerM4 Tornado micro-XRF that is housed at the Institute for Geoscience at Aarhus University. The X-rays are generated via a Rh tube at 50 kV and 600 pA current, and the mapping was undertaken with a spot size 25 μm and scan speed of 1 mm/s. The sample was also carbon-coated and then analysed using a TecScan scanning electron microscope (SEM) that is also housed in the Institute for Geoscience, Aarhus University. This instrument was operated with an emission of 20 kV and a beam current of 20 nA, with the current measured and calibrated on copper tape. The operating distance was maintained at precisely 15 mm. SEM data were standardised to factory standards, and our process is capable of producing high quality data comparable with microprobe-derived data (see Pedersen *et al.* (2025) for further discussion).

Results

Dueodde is a rounded meteorite with a thin black fusion crust that has been partially abraded to locally expose the pale interior (Fig. 1). The meteorite has a regmaglypt on one surface. Petrological characterisation of the meteorite shows that it is typically medium to coarse-grained (Fig. 2a) with a high proportion of S-rich and Ni-rich phases (Fig. 2b). Furthermore, the meteorite contains chondrules set in an olivine and orthopyroxene-dominated matrix with lesser feldspar, clinopyroxene, kamacite, troilite, taenite, chromite, merrillite, and apatite (Fig. 3a, 3b). Olivine and orthopyroxene grains are typically up to 500 μm in length, with clinopyroxene tending to range from 200 μm to 10 μm. Plagioclase is scattered throughout the matrix and tends to be small (around 100 μm or less) and anhedral. As we did not analyse the structural state of the feldspar, it is unclear whether it is crystalline plagioclase or maskelynite (feldspar-composition shock glass). Kamacite and chromite are the most abundant non-silicate phases, with lesser taenite and troilite also present. These grains can be larger than silicate phases and are in some cases up to almost 1 mm in diameter. Phosphate minerals are present in minor quantities and again range in size from 10 μm grains scattered throughout the matrix to larger ~500 μm crystals.

SEM analyses show matrix olivine and pyroxene grains are Fe-poor, with an average olivine composition of $Fa_{16\text{-}20}$ and an orthopyroxene composition of $En_{81\text{-}82}Fs_{17\text{-}18}Wo_{1\text{-}2}$ (Appendix 1). Olivine analyses fall in the very small range of $Fa_{19\text{-}20}$. The composition of matrix feldspar is oligoclase with an average compositional range of $Ab_{81\text{-}84}An_{12\text{-}13}Or_{4\text{-}7}$ (Appendix 1).

Chondrules

Chondrules in Dueodde range in size in 2D from approximately 200 μm to ~3 mm diameter (Fig. 4a). They display a variety of textures, including porphyritic (Fig. 4b), barred olivine-plagioclase (Fig. 4c), and radial to barred olivine-orthopyroxene (Fig. 4d). The chondrules are composed of assemblages comprising combinations of plagioclase, olivine, orthopyroxene, and clinopyroxene, with minor accessory chromite and apatite. Fe-rich phases such as kamacite, taenite, and troilite generally occur in only small proportions at the rims within the barred and radial chondrules. In the porphyritic chondrules, they constitute a minor phase.

Alongside mineral analyses, individual chondrules were mapped and bulk compositions were determined by the Aztec program (https://nano.oxinst.com/products/aztec/) for these map areas. Results show the chondrules typically have high SiO_2 (av. 47 wt%), MgO (26 wt%), and FeO (av. 14 wt%), but also indicates low S and Ni concentrations (Appendix 2). While we observe compositional diversity in the chondrules, no systematic difference between chondrule morphological types was identified. The EDS analyses indicate that chondrule olivine is Fe-poor, with an average composition of $Fa_{19\text{-}20}$ (Appendix 1). The second most common mineral in the chondrules is low-Ca orthopyroxene with the composition of $En_{81\text{-}82}Fs_{17\text{-}18}Wo_{1\text{-}2}$ (Appendix 1) with the standard deviation of ± 0.2-0.3. Feldspar occurring in radial textural chondrules has the composition of $Ab_{81\text{-}82}An_{11\text{-}13}Or_{5\text{-}8}$ (oligoclase; Appendix 1). No primary glass was identified.

Fusion crust

The fusion crust is visible along part of the outer edge of the meteorite as a relatively thin layer consisting mainly of glass and containing minute quenched crystals of an uncertain composition, grains of millerite, and vesicles (Figs 1, 2a, 5). The thickness is variable, but reaches 50 to 150 μm. Feldspar, orthopyroxene, and clinopyroxene immediately adjacent to the fusion crust have long fractures that are filled with metal (Fig. 5). This zonation has been observed in the narrow zone adjacent to the fusion crust in other meteorites (e.g., Scott *et al.* 2023).

Discussion

Classification of the Dueodde

In this work, we follow the classification scheme for chondrites outlined in Davis (2005). This is normally done to group meteorites that originated from the same parent body. The principal distinction in meteorite taxonomy is between chondrites and achondrites: the former represents material that has not been part of a differentiated body, whilst the latter has. A meteorite class, which in the case of chondrites is ordinary, carbonaceous or enstatite is then assigned based on the dominant composition of the rock, and chosen based on geochemical parameters. A shock metamorphic grade and weathering state may then also be assigned.

Within Dueodde, the presence of intact porphyritic (Fig. 4b) chondrules alongside barred (Fig. 4c) and radial (Fig. 4d) varieties, coupled with the dominant

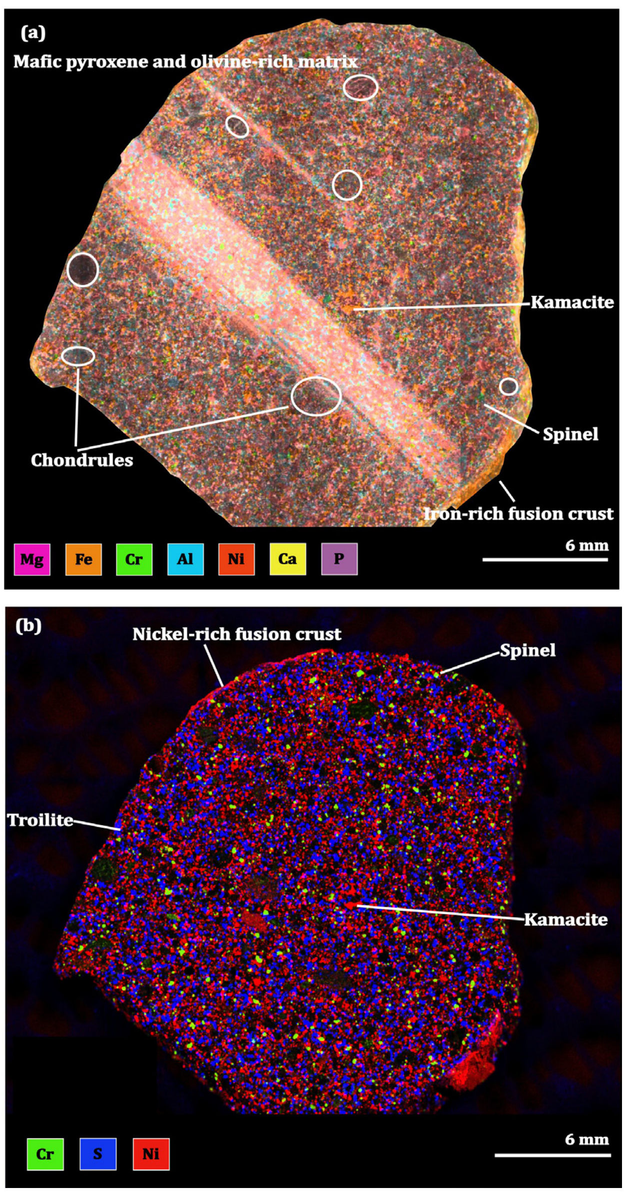

Fig. 2. MicroXRF false-colour images of Dueodde. **a:** Chemical element map of the slice of meteorite. The fusion crust is highlighted on the right-hand side. Well-preserved chondrules are evident as metal-free areas. The prominent mark across the middle of the sample is an unpolished saw mark. **b:** Cr-S-Ni element map highlighting metal distribution.

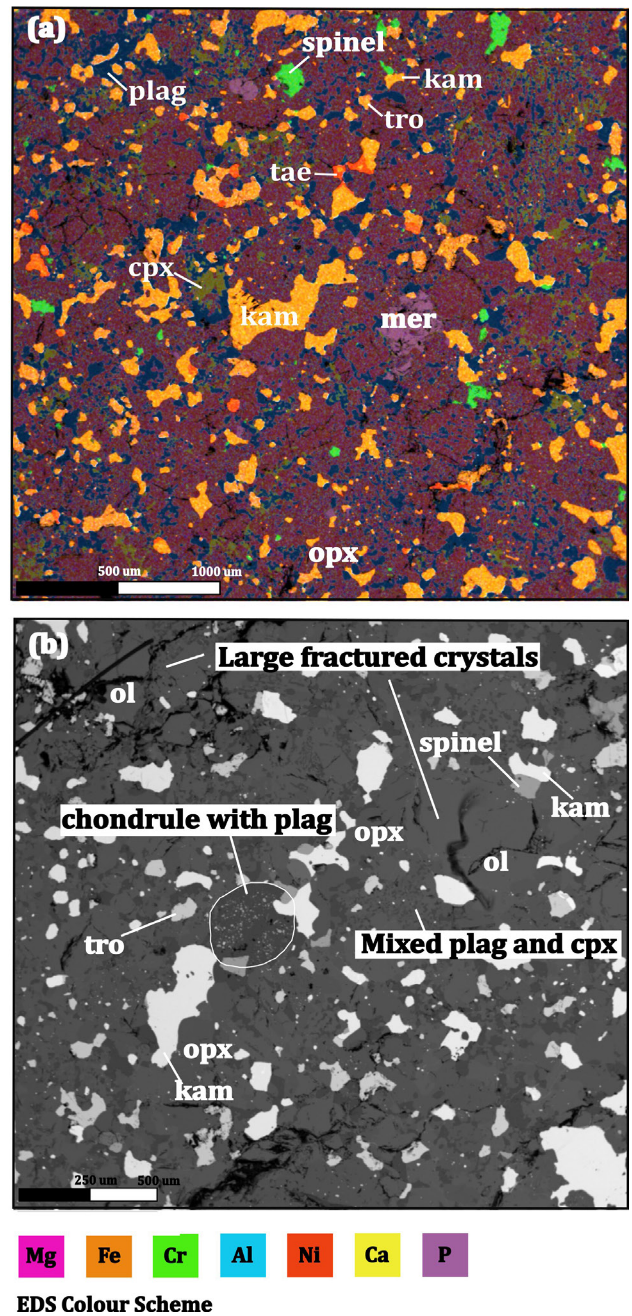

Fig. 3. a: EDS image of Dueodde; **b**: BSE image. Major mineral phrases are noted alongside textural examples (chondrules, fractures). Key: cpx = clinopyroxene; kam = kamacite; mer = merrilite; opx = orthopyroxene; ol = olivine; plag = plagioclase; tae = taenite; tro = troilite.

olivine-pyroxene-plagioclase mineralogy, demonstrates that Dueodde is from an undifferentiated ordinary chondrite parent body. The Fa# of olivine (Fa_{19-20}) and ferrosilite in orthopyroxene (Fs_{17-18}) falls within the range of an H-chondrite, which is $Fa_{17.3-20.2}$ or $Fa_{16.1-19.4}$ for olivine and $Fs_{17.9-21.7}$ for pyroxene (Rubin 1990; Keil & Fredriksson 1964). The average feldspar composition ($Ab_{81-84}An_{12-13}Or_{4-7}$ for matrix plagioclase, and $Ab_{81-82}An_{11-13}Or_{5-8}$ for chondrules) is also like that given for H-chondrites ($Ab_{82}An_{12}Or_{6}$; van Schmus & Ribbe 1968).

We use the classification scheme of Krot *et al.* (2014) to assign a petrologic type to Dueodde. The olivine-pyroxene dominant matrix composition with a medium to coarse grained texture, alongside the homogeneous olivine and pyroxene compositions suggest a petrologic type of 4-6. Chondrules are still well defined in many cases (Fig. 4), which excludes a type 6 classification, but are not so sharply defined as one would expect for a class 3 or 4 meteorite. We therefore classify Dueodde as being of petrologic type 5, with readily delineated, but not sharp, chondrules, in accordance with the Meteoritical Bulletin classification.

Discriminating the shock metamorphic state is difficult here, as we have not been able to distinguish between crystalline and glass (maskelynite) plagioclase, a primary factor in assessing shock state (Stoffler *et al.* 2018). Weak to absent mosaicism and irregularity in fractures tentatively leads to the conclusion of a shock state of at least 3–4. Weathering appears to be relatively minor, with only minor oxidation of interior metal grains and veins. A few oxidised veins are seen on the surface of the meteorite (Fig. 1), and we therefore assign an overall weathering state of W1 following Wlotzka (1993). The chondrules in Dueodde show a clear depletion in metal relative to the matrix (Figs 2, 4). The absence of metal in chondrules is not a newly recognised feature but is generally thought to result from expulsion while the chondrule was molten in the solar nebula before incorporation in the parent body (e.g., Jacquet, 2021). The distribution of the metals in Dueodde, and the small variation in compositions, indicates that although mineral equilibrium has been achieved of grade 5, textural geological evidence of processes from very early in the Solar System are still preserved.

Our H5 interpretation can be compared with other H5 examples as a check of our classification. For example, Dergaon, which fell in India in 2001 (Shukla *et*

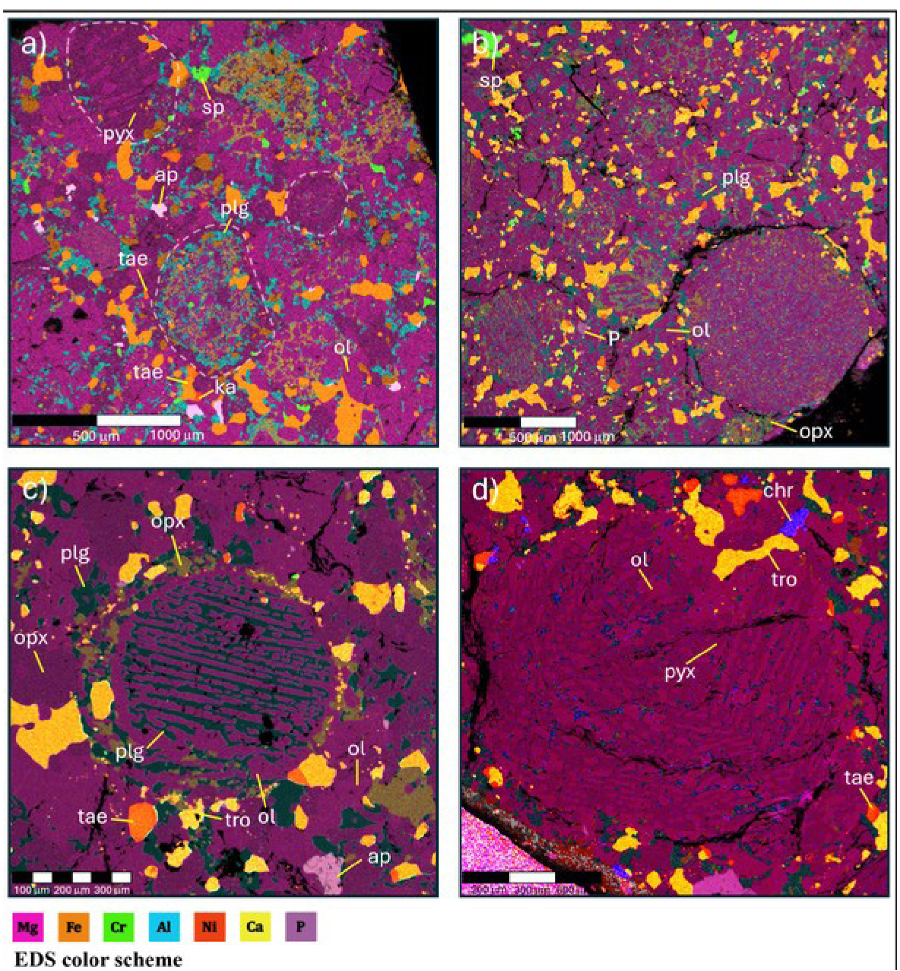

Fig. 4. False-coloured element maps of chondrules in Dueodde showing different porphyritic (**b**), barred (**c**) and radial (**d**). Colours have been slightly enhanced in Fig. 4d.

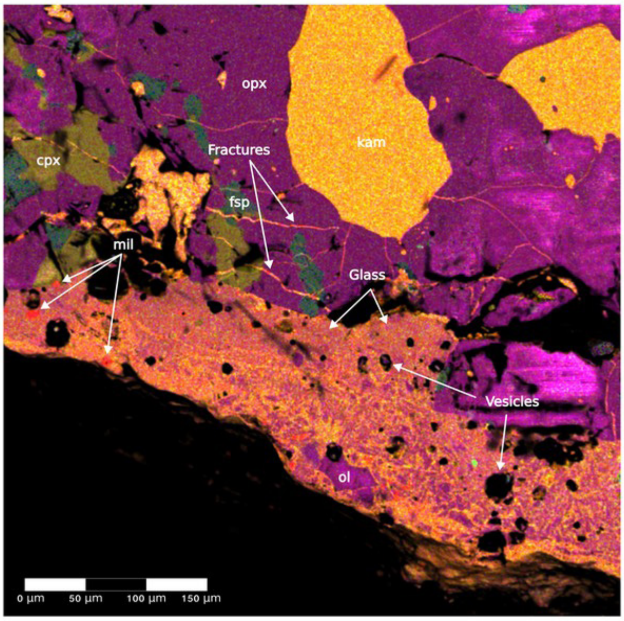

Fig. 5. False-coloured close-up EDS image of the fusion crust on Dueodde.

al. 2005), shows an overall similar mineral assemblage made up of olivine, orthopyroxene, calcic pyroxene, Na-rich plagioclase, chromite, and metallic phases (mostly kamacite with rare occurrences of troilite and taenite). The Fa_{20} for olivine and $Fs_{18\text{-}19}$ for orthopyroxene in Dergaon (Shukla *et al.* 2005) overlap with Dueodde compositions (Fig.6). The chondrules in both meteorites show a uniform chemical composition with the matrix, indicating equilibrium of the minerals across the rocks. Many of the chondrule textures are similar between the two meteorites, although Dergaon chondrules also exhibit features such as reaction rims and exsolution lamellae. The chondrules in Dergaon are measured to be between 0.1 to 1 mm in diameter, which is substantially smaller than the range of those in Dueodde. Texturally, Dergaon is reported to have a fine-grained interior, which contrasts with the medium to coarse-grained interior of Dueodde. In terms of weathering degree, it is not possible to directly compare Dueodde to the Dergaon meteorite, as Dergaon was soaked in water, which caused the fusion crust and exposed interior to rust before classification. Despite the textural differences, a classification of H5 remains appropriate for Dueodde.

Comparison with other Danish H-chondrites

The images and data presented for Dueodde now supplement two other Danish H-chondrites, which likely come from the same parent body: the H5/6 Ejby (Haack *et al.* 2019) and H6 Aarhus (Pedersen *et al.* 2025). They are grouped together here simply because they landed in Denmark and thus the interested reader could see them altogether in the Copenhagen National History Museum. All three are composed of a consistent mineral assemblage dominated by olivine, orthopyroxene, and plagioclase as well as metal and sulphide phases such as kamacite and troilite. Aarhus preserves brecciated textures that have been metamorphosed, which are not evident in Ejby or Dueodde. Their mineral chemistries are similar, with Dueodde's average olivine compo-

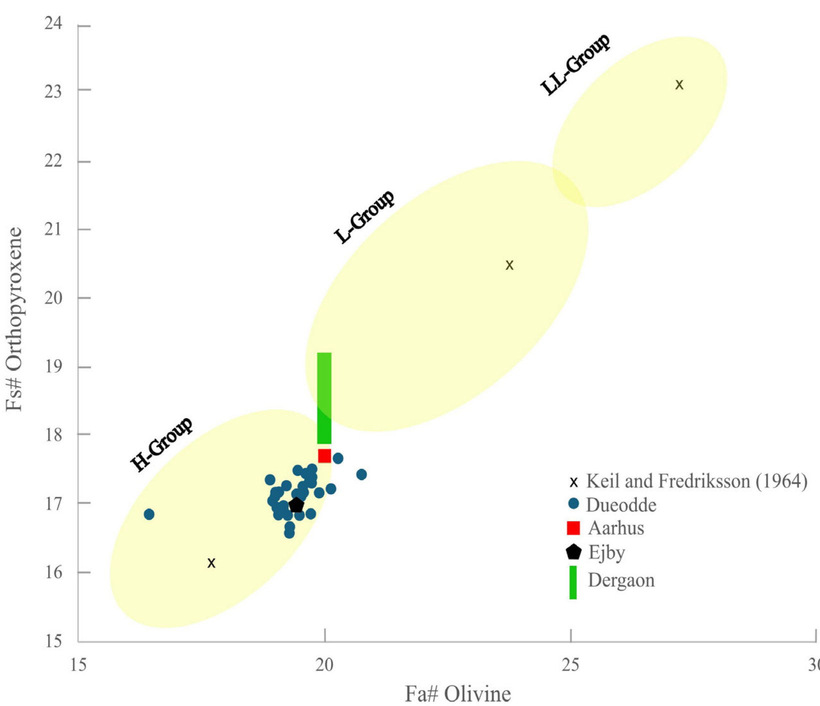

Fig. 6. Composition of Dueodde versus other chondrites mentioned in the text. The Keil & Fredriksson (1964) data are the chondrite group averages; data for Aarhus is sourced from Pederson *et al.* (2025); that of Ejby is from Haack *et al.* (2019); and Dergaon data are from Shukla *et al.* (2005).

sition being Fa_{19-20} and orthopyroxene Fs_{17-18} aligning with Ejby's $Fa_{19.3}/Fs_{16.9}$ and Aarhus's $Fa_{19.9}/Fs_{17.6}$ (Fig. 6). However, their petrological types reflect varying degrees of thermal metamorphism: Aarhus, a type 6, is highly equilibrated with poor chondrule delineation, whereas Dueodde and Ejby have experienced moderate metamorphism and chondrules are still readily discernible. Another difference is the shock histories, with H5 Dueodde potentially having an intermediate S3–4 shock state, and H5/6 Ejby being S2 (weakly shocked) and H6 Aarhus being S5 (strongly shocked).

Traditionally different metamorphic grades of classes of meteorite were attributed to excavation from different distances from the centre of the parent body; however, cooling rates do not support this model and the now favoured alternative is that the H chondrite parent body was once concentrically metamorphically zoned but then disrupted early in the Solar System history and probably recombined as a rubble pile of accumulated metamorphosed material (Blackburn *et al.* 2017). Thus, despite the characterisation of these Danish meteorites as H5 to H6, the relative actual location on the last parent body remains unclear, which may explain the lack of correlation between shock state and metamorphic grade.

Conclusion

Dueodde is a small meteorite that was recovered from a roof cavity in a summerhouse in Dueodde on the Danish island of Bornholm. This meteorite, weighing just 75 g, displays a thin black fusion crust surrounding a pale-coloured interior. Microscopic analysis shows a metamorphic olivine-pyroxene-plagioclase/maskelynite matrix that is rich in kamacite, along with lesser taenite and troilite, enclosing barred, radial, and porphyritic chondrules. Scanning electron microscope element maps clearly reveal the chondrules to be depleted in metal relative to the matrix, interpreted to be related to processes within the solar nebula before parent body formation. Our first-published olivine, orthopyroxene, and plagioclase mineral compositions, as well as the first microscopic images and element maps, confirm classification of Dueodde as a moderately metamorphosed high iron ordinary chondrite (H5).

Acknowledgments

We thank F. Wright and M. Bizzarro for the loan of the meteorite, and M. Bizzarro for permission to use the photo in Figure 1. This article was written as part of the Tectonics and Petrology of Earth and the Solar System course at Aarhus University, which was supported by O. R. Clausen. We thank Henning Haack and William Hyde for reviewing the text and Tod Waight for editorial handling.

References

Blackburn, T., Alexander, C.M.D., Carlson, R. & Elkins-Tanton, L.T. 2017: The accretion and impact history of the ordinary chondrite parent bodies. Geochimica et Cosmochimica Acta 200, 201–217. https://doi.org/10.1016/j.gca.2016.11.038

Davis, A. M. (Ed., 2005: Meteorites, comets, and planets: Treatise on Geochemistry, Volume 1. Elsevier.

Haack, H. et al. 2019: Ejby—A new H5/6 ordinary chondrite fall in Copenhagen, Denmark. Meteoritics & Planetary Science 54, 1853–1869. https://doi.org/10.1111/maps.13344

Jacquet, E. 2021: Collisions and compositional variability in chondrule-forming events. Geochimica et Cosmochimica Acta 296, 18–37. https://doi.org/10.1016/j.gca.2020.12.025

Keil, K. & Fredriksson, K. 1964: The iron, magnesium, and calcium distribution in coexisting olivines and rhombic pyroxenes of chondrites. Journal of Geophysical Research 69, 3487–515. https://doi.org/10.1029/JZ069i016p03487

Krot, A.N., Keil, K., Scott, E.R.D., Goodrich, C.A, & Weisberg, M.K. 2014: Classification of meteorites and their genetic relationships. In: Holland, H.D. & and Turekian, K.K.: Treatise on Geochemistry Volume 1: Meteorites and Cosmochemical Processes, 1–64. Amsterdam: Elsevier.

Pedersen, M.C., Waight, T.E. & Scott, J.M. 2025: The H6 Aarhus meteorite breccia: A new look at an old rock. Bulletin of the Geological Society of Denmark 74, 209–217. https://doi.org/10.37570/bgsd-2025-74-11

Rubin, A.E. 1990: Kamacite and olivine in ordinary chondrites: Intergroup and intragroup relationships. Geochimica et Cosmochimica Acta 54, 1217–1232. https://doi.org/10.1016/0016-7037(90)90148-E

Scott, J.M., Negrini, M., Faure, K., Palmer, M.C., Knaack, D.R. & Leybourne, M.I. 2023: Multi-zone fusion crust formation and classification of the 2004 Auckland meteorite (L6, S5, and W0). Meteoritics & Planetary Science 58, 328–340. https://doi.org/10.1111/maps.13955

Shukla, P.N. et al. 2005: The Dergaon (H5) chondrite: Fall, classification, petrological and chemical characteristics, cosmogenic effects, and noble gas records. Meteoritics & Planetary Science 40, 627–637. https://doi.org/10.1111/j.1945-5100.2005.tb00967.x

Stöffler, D., Hamann, C. & Metzler, K. 2018: Shock metamorphism of planetary silicate rocks and sediments: Proposal for an updated classification system. Meteoritics & Planetary Science 53, 5–49. https://doi.org/10.1111/maps.12912

Van Schmus, W.R. & Ribbe, P.H. 1968: The composition and structural state of feldspar from chondritic meteorites. Geochimica et Cosmochimica Acta 32, 1327–1342. https://doi.org/10.1016/0016-7037(68)90032-X

Wlotzka, F. 1993: A weathering scale for the ordinary chondrites. Meteoritics 28, 460.

Appendix 1. Average chemical composition of selected matrix and chondrule mineral phases in Dueodde

	Spectrum 29 Matrix	Spectrum 57 Matrix	Spectrum 31 Matrix	Spectrum 7 Matrix	Spectrum 34 Matrix	Spectrum 47 Matrix	Spectrum 36 Matrix	Spectrum 9 Matrix	Spectrum 25 Chondrule	Spectrum 13 Chondrule	Spectrum 16 Chondrule	Spectrum 21 Chondrule	Spectrum 23 Chondrule	Spectrum 43 Chondrule	Spectrum 12 Chondrule	Spectrum 39 Chondrule	Spectrum 60 Chondrule rim
SiO_2	38.56	38.57	38.61	38.63	38.81	38.86	38.93	38.97	38.42	38.62	38.62	38.62	38.66	38.66	38.73	38.95	38.62
TiO_2	0.00	0.00	0.00	0.00	0.00	0.00	0.00	0.00	0.00	0.00	0.00	0.00	0.00	0.00	0.00	0.00	0.00
Al_2O_3	0.00	0.00	0.00	0.00	0.00	0.00	0.00	0.00	0.00	0.00	0.00	0.00	0.00	0.00	0.00	0.00	0.00
FeO	17.95	18.41	18.61	18.24	18.41	18.65	18.43	18.32	18.05	18.28	18.03	18.13	17.84	18.10	18.12	18.63	18.40
MnO	0.48	0.52	0.47	0.53	0.49	0.49	0.47	0.47	0.48	0.48	0.45	0.46	0.47	0.49	0.46	0.47	0.46
MgO	42.24	42.07	42.48	42.53	42.41	42.65	42.63	42.52	42.12	42.18	42.15	42.30	42.36	41.98	42.31	42.56	42.34
CaO	0.00	0.00	0.00	0.00	0.00	0.00	0.00	0.00	0.00	0.00	0.00	0.00	0.00	0.09	0.00	0.00	0.00
Na_2O	0.00	0.00	0.00	0.00	0.00	0.00	0.00	0.00	0.00	0.00	0.00	0.00	0.00	0.00	0.00	0.00	0.00
K_2O	0.00	0.00	0.00	0.00	0.00	0.00	0.00	0.00	0.00	0.00	0.00	0.00	0.00	0.00	0.00	0.00	0.00
Total	99.23	99.57	100.17	99.93	100.12	100.65	100.46	100.28	99.07	99.56	99.25	99.51	99.33	99.32	99.62	100.61	99.82
Oxygens	4	4	4	4	4	4	4	4	4	4	4	4	4	4	4	4	4
Si	0.99	0.99	0.99	0.99	0.99	0.99	0.99	0.99	0.99	0.99	0.99	0.99	0.99	0.99	0.99	0.99	0.99
Al	0.00	0.00	0.00	0.00	0.00	0.00	0.00	0.00	0.00	0.00	0.00	0.00	0.00	0.00	0.00	0.00	0.00
Ti	0.00	0.00	0.00	0.00	0.00	0.00	0.00	0.00	0.00	0.00	0.00	0.00	0.00	0.00	0.00	0.00	0.00
Fe	0.39	0.40	0.40	0.39	0.39	0.40	0.39	0.39	0.39	0.39	0.39	0.39	0.38	0.39	0.39	0.40	0.39
Mn	0.01	0.01	0.01	0.01	0.01	0.01	0.01	0.01	0.01	0.01	0.01	0.01	0.01	0.01	0.01	0.01	0.01
Mg	1.62	1.61	1.62	1.62	1.61	1.62	1.62	1.61	1.62	1.61	1.62	1.62	1.62	1.61	1.62	1.61	1.62
Ca	0.00	0.00	0.00	0.00	0.00	0.00	0.00	0.00	0.00	0.00	0.00	0.00	0.00	0.00	0.00	0.00	0.00
Na	0.00	0.00	0.00	0.00	0.00	0.00	0.00	0.00	0.00	0.00	0.00	0.00	0.00	0.00	0.00	0.00	0.00
K	0.00	0.00	0.00	0.00	0.00	0.00	0.00	0.00	0.00	0.00	0.00	0.00	0.00	0.00	0.00	0.00	0.00
Total	3.01	3.01	3.01	3.01	3.01	3.01	3.01	3.01	3.01	3.01	3.01	3.01	3.01	3.01	3.01	3.01	3.01
Fa#	19.3	19.7	19.7	19.4	19.6	19.7	19.5	19.5	19.4	19.6	19.4	19.4	19.1	19.5	19.4	19.7	19.6
Fs#																	
Wo#																	
Ab#																	

Appendix 1. Continued

	Spectrum 8 Matrix	Spectrum 56 Matrix	Spectrum 38 Matrix	Spectrum 33 Matrix	Spectrum 32 Matrix	Spectrum 30 Matrix	Spectrum 22 Matrix	Spectrum 18 Matrix	Spectrum 17 Matrix	Spectrum 10 Matrix	Spectrum 42 Chondrule	Spectrum 40 Chondrule	Spectrum 27 Chondrule	Spectrum 26 Chondrule	Spectrum 20 Matrix	Spectrum 45 Matrix	Spectrum 28 Matrix	Spectrum 37 Matrix	Spectrum 24 Chondrule	Spectrum 15 Chondrule
SiO_2	56.03	55.67	56.31	56.45	56.56	55.13	55.53	55.10	55.40	55.85	55.28	55.45	55.32	55.34	63.67	64.00	64.25	64.49	63.94	64.07
TiO_2	0.20	0.16	0.25	0.18	0.06	0.25	0.19	0.21	0.18	0.18	0.26	0.32	0.21	0.18	0.00	0.00	0.00	0.00	0.00	0.00
Al_2O_3	0.23	0.20	0.21	0.24	0.11	0.29	0.23	0.23	0.21	0.24	0.28	0.41	0.25	0.24	21.88	22.05	22.04	21.91	21.94	21.84
FeO	11.73	11.72	11.80	11.71	11.65	11.48	11.33	11.83	11.45	11.62	11.56	11.56	11.44	11.43	0.67	1.06	0.33	0.59	0.86	0.58
MnO	0.50	0.56	0.53	0.52	0.54	0.48	0.54	0.49	0.52	0.50	0.54	0.53	0.50	0.49	0.00	0.00	0.00	0.00	0.00	0.00
MgO	31.07	30.77	31.28	31.22	31.17	30.79	30.76	30.66	30.80	31.10	30.62	30.64	30.80	30.65	0.00	0.00	0.00	0.30	0.37	0.11
CaO	0.69	0.65	0.60	0.72	0.79	0.66	0.80	0.57	0.64	0.66	0.65	0.74	0.63	0.71	2.56	2.54	2.54	2.82	2.46	2.49
Na_2O	0.00	0.00	0.00	0.00	0.00	0.00	0.00	0.00	0.00	0.00	0.00	0.00	0.00	0.00	9.24	9.32	9.55	8.99	9.50	9.43
K_2O	0.00	0.00	0.00	0.00	0.00	0.00	0.00	0.00	0.00	0.00	0.00	0.00	0.00	0.00	1.13	1.09	0.83	1.46	0.90	1.06
Total	100.45	99.73	100.98	101.04	100.88	99.08	99.38	99.09	99.20	100.15	99.19	99.65	99.15	99.04	99.15	100.06	99.54	100.56	99.97	99.58
Oxygens	6	6	6	6	6	6	6	6	6	6	6	6	6	6	8	8	8	8	8	8
Si	1.98	1.98	1.98	1.98	1.99	1.97	1.98	1.97	1.98	1.98	1.98	1.97	1.98	1.98	2.85	2.84	2.85	2.85	2.84	2.85
Al	0.01	0.01	0.01	0.01	0.00	0.01	0.01	0.01	0.01	0.01	0.01	0.02	0.01	0.01	1.15	1.15	1.15	1.14	1.15	1.14
Ti	0.01	0.00	0.01	0.00	0.00	0.01	0.01	0.01	0.00	0.00	0.01	0.01	0.01	0.00	0.00	0.00	0.00	0.00	0.00	0.00
Fe	0.35	0.35	0.35	0.34	0.34	0.34	0.34	0.35	0.34	0.34	0.35	0.34	0.34	0.34	0.03	0.04	0.01	0.02	0.03	0.02
Mn	0.01	0.02	0.02	0.02	0.02	0.01	0.02	0.01	0.02	0.01	0.02	0.02	0.02	0.01	0.00	0.00	0.00	0.00	0.00	0.00
Mg	1.63	1.63	1.64	1.63	1.63	1.64	1.63	1.64	1.64	1.64	1.63	1.62	1.64	1.63	0.00	0.00	0.00	0.02	0.02	0.01
Ca	0.03	0.02	0.02	0.03	0.03	0.03	0.03	0.02	0.02	0.03	0.02	0.03	0.02	0.03	0.12	0.12	0.12	0.13	0.12	0.12
Na	0.00	0.00	0.00	0.00	0.00	0.00	0.00	0.00	0.00	0.00	0.00	0.00	0.00	0.00	0.80	0.80	0.82	0.77	0.82	0.81
K	0.00	0.00	0.00	0.00	0.00	0.00	0.00	0.00	0.00	0.00	0.00	0.00	0.00	0.00	0.06	0.06	0.05	0.08	0.05	0.06
Total	4.01	4.01	4.01	4.01	4.01	4.02	4.01	4.02	4.01	4.01	4.01	4.01	4.01	4.01	5.01	5.02	5.01	5.01	5.02	5.01
Fa#																				
Fs#	17.3	17.4	17.3	17.1	17.1	17.1	16.9	17.6	17.0	17.1	17.3	17.2	17.0	17.1						
Wo#	1.3	1.2	1.1	1.4	1.5	1.3	1.5	1.1	1.2	1.2	1.2	1.4	1.2	1.4						
Ab#															81.1	81.5	83.0	78.1	83.0	82.0

Appendix 2. Average chondrule bulk compositions. Data are normalised to 100 %

	SiO_2	Ti_2O	Al_2O_3	FeO	MnO	MgO	CaO	K_2O	Na_2O	Cr_2O_3	P_2O_5	S	NiO	Total
barred	51.01	0.15	0.24	13.79	0.48	32.92	0.54	0.00	0.09	0.22	0.00	0.56	0.00	100
barred	48.06	0.00	9.50	11.36	0.26	24.08	1.79	0.36	3.69	0.00	0.77	0.13	0.00	100
porp	47.78	0.22	2.74	15.58	0.31	19.33	8.98	0.11	1.35	0.37	0.00	2.32	0.91	100
porp	50.40	0.13	0.88	13.28	0.45	33.13	1.07	0.00	0.34	0.33	0.00	0.00	0.00	100
porp	35.37	0.19	0.48	19.01	0.50	39.82	0.05	0.00	0.00	4.59	0.00	0.00	0.00	100
porp	47.46	0.10	5.98	12.07	0.31	24.08	4.48	0.23	2.49	0.48	0.00	2.17	0.14	100
porp	51.37	0.15	2.66	11.78	0.42	27.74	2.82	0.10	1.10	0.45	0.29	0.99	0.14	100
porp	47.27	0.12	9.45	14.91	0.16	12.84	5.03	0.36	4.24	0.25	0.00	4.67	0.70	100